Neutrophil arrest in myocardial capillaries drives hypoxia and impairs diastolic function in a mouse model of heart failure with preserved ejection fraction

David M. Small[1]*, Anne E. Buglione[1,2]*, Nathaniel H. Allan-Rahill[1], Tyler Locke[1], Laila M. Abd Elmagid[1], Soseh Hovasapian[1], Rachel Kim[1], Adina A. Mistry[1], Sofia A. Vaquerano[1], Chris B. Schaffer[1], Nozomi Nishimura[1]

* co-first authors

Contact: nn62@cornell.edu

Affiliation:
1. Nancy E. and Peter C. Meinig School of Biomedical Engineering, Cornell University, Ithaca, New York, United States.
2. College of Veterinary Medicine, Cornell University, Ithaca, New York, United States

ABSTRACT

Myocardial blood flow deficits in heart failure with preserved ejection fraction (HFpEF) patients and related animal models have been recognized for decades, but the underlying mechanisms and resulting consequences for HFpEF pathogenesis remain poorly understood. Using intravital cardiac microcopy in a 'two-hit' mouse model of HFpEF, we identified an increased number of neutrophils in capillaries slow moving orstalled, blocking blood flow, as compared to control mice. Administration of antibodies against the neutrophil marker Ly6G reduced the number of arrested neutrophils in myocardial capillaries, leading to both a reduction in myocardial tissue hypoxia and improvement in diastolic function and exercise tolerance. This study identifies a previously uncharacterized cellular mechanism that explains myocardial blood flow deficits in mouse models of HFpEF, and demonstrates that improving myocardial blood flow improves heart function. Restoring myocardial perfusion by preventing neutrophil arrest in coronary capillaries may provide a strategy for improving heart function in HFpEF patients.

INTRODUCTION

Heart failure with preserved ejection fraction (HFpEF) is primarily characterized by an impaired filling capacity of the heart (diastolic dysfunction), and presents with a complex interplay of factors including reduced cardiac reserve, endothelial dysfunction, ventricular stiffening, and hypertension.[1] The majority of therapies that have improved morbidity and mortality in heart failure with reduced ejection fraction (HFrEF) have proven ineffective against HFpEF.[2,3] Only one treatment for HFpEF has been shown to reduce the risk of hospitalization, yet does not reduce mortality.[4] Development of novel, rationally targeted therapeutic approaches in HFpEF mandates the development of a more complete understanding of alterations in cellular homeostasis occurring in this condition.

Multiple studies show that blood flow is decreased in myocardial tissue in HFpEF even in the absence of major arterial obstruction.[5-9] The cause of this myocardial perfusion deficit is still unknown. Reduced coronary flow reserve, defined as the ratio of coronary flow before and after stimulation, is common in HFpEF patients.[5-7] Additionally, studies in HFpEF patients without obstructive coronary artery disease demonstrate increased microvascular resistance under stimulation,[8] decreased volumetric flow,[5] and reduced myocardial oxygen supply with exercise compared to healthy controls.[9] Structural loss of capillaries via rarefaction is noted in patients[10] and in animal models[11] of HFpEF, and is thought to be related to inflammation.[12] The microvasculature is often referred to as a likely culprit, although specifics are unclear.

HFpEF is thought to have differing etiology than HFrEF, with a greater contribution of systemic inflammation and microvascular dysfunction driven by cardiovascular and metabolic risk factors which contribute to low grade, chronic, systemic inflammation.[13,14] It is not clear how inflammation leads to HFpEF,

but multiple lines of evidence suggest a contribution of dysfunction of the coronary microvasculature. [15] Endothelial activation is increased in HFpEF, indicated by the expression of vascular adhesion molecules and decreased bioavailability of nitric oxide (NO).[8,16-18] Evidence supports immune and inflammatory cell infiltration of the heart, including neutrophils, in human and animal HFpEF[19] and HFrEF studies[20] of post-mortem tissue. However, the behavior of these cells within the cardiac microcirculation and how their recruitment impacts coronary microcirculatory dynamics have not been defined.

The convergence of the coronary microcirculation, inflammatory cells, and cardiomyocyte function in HFpEF phenotype requires *in vivo* study. Intravital microscopy is the uniquely able to show the dynamic interactions of circulating leukocytes within the microvasculature during inflammation.[21-25] Recent technical advances have overcome the unique set of challenges associated with imaging the live beating heart in mouse models of disease.[26-29,30] This enables direct visualization of dynamic processes such as blood flow, which are impossible to study in cultured or extracted tissues. These imaging capabilities provide a link between microvascular dysfunction, inflammation, and reduced blood flow in the HFpEF heart. Using intravital cardiac MPM in mouse models of heart failure, we show that neutrophils arrest in coronary capillaries to reduce microvascular blood flow, contributing to cardiac remodeling and dysfunction. The elimination of these stalled capillaries drives rapid improvement of hypoxia and diastolic stiffness, even without altering hypertrophy.

RESULTS

Two-photon intravital imaging shows stalled capillaries plugged by neutrophils in HFpEF. Male and female C57Bl/6 mice were subjected to the HFpEF induction protocol of a high-fat diet and L-NAME in drinking water for 15 weeks ('HFpEF') and compared to controls that remained on the normal chow diet and water. HFpEF mice developed hypertrophy, as measured by the ratio of heart weight to tibia length, while left ventricular (LV) ejection fraction (Fig. 1a-b) was unchanged as previously reported (Supplementary Figure 1). (Supplementary Figure 1). To investigate the interplay between microvasculature, leukocyte activity, and myocardial capillary blood flow in HFpEF, we used intravital cardiac two-photon microscopy to image the left ventricular epicardial microvasculature [26,27,3] Plasma was labeled with retro-orbital injection of dextran-conjugated dyes or quantum dots. Erythrocytes and leukocytes are visible as regions of excluded labeling, which appear as dark patches within the vessel. Use of Catchup$^{IVM\text{-}Red}$ mice, which express TdTomato on the surface of neutrophils,[31] and heterozygous knock-in mice (Cx3Cr1$^{GFP/+}$ x CCR2$^{RFP/+}$)[30,31], which express green and red fluorescent proteins (GFP and RFP) in monocytes and macrophages, allowed identification of specific classes of leukocytes. Labeled neutrophils and monocytes within capillaries were manually tracked in image stacks (100 frames x 30 fps from ~20 to 200 μm below the left ventricle surface with 2 μm steps). Due to the periodic motion from heartbeat and breathing at approximately 5-6 Hz and 1.6 Hz, capillaries appear repeatedly in the imaging stack and are recognizable over about 1-2 minutes, allowing the visualization of neutrophils and monocytes as they transited through the capillary beds. While the majority of neutrophils and monocytes were visible for less than ~2 s, many cells took longer to traverse the imaging region. These stalled neutrophils and monocytes appeared in the same location over multiple image frames (Fig. 1c-d).

In Catchup mice, we measured the time each neutrophil was visible within the image stack (Fig. 1e). To reduce the variability due to the differing amount of time a particular capillary is visible in the image volume we sampled over multiple image stacks per mouse. The distribution of times differed between HFpEF and control with a greater proportion of neutrophils in HFpEF persisting for longer times ($p<0.0001$ Kolmogorov–Smirnov (KS) test, Fig. 1e). The total amount of time that a neutrophil was present in the image stack and the visible time per cell were increased by 1.7x and 3x (Fig. 1f and 1g) in HFpEF relative to control mice. Similar experiments using Cx3Cr1$^{GFP/+}$ x CCR2$^{RFP/+}$ mice with labeled monocytes[22,30,32] revealed no difference between the monocytes of HFpEF and control in the distribution of time in the image stack ($p= 0.73$ KS test, Fig. 1f). Cells expressing only CCR2-RFP were exceedingly rare (<1/min) and the observed circulating cells predominantly expressed both Cx3Cr1-GFP and CCR2-RFP, so we tracked cells expressing GFP as a measure of monocytes. Observed circulating monocytes were on average less common than neutrophils, slower, and associated with a longer dwell time, regardless of treatment group (Figure 1g-h). The frequency of slow-moving leukocytes was similarly elevated in 26 week-old ApoE$^{-/-}$ mice

fed a HFD for 20 weeks and we found the number of stalled capillaries was doubled compared to control (age-matched wildtype mice on standard diet (Supplementary Figure 2 and 3)).

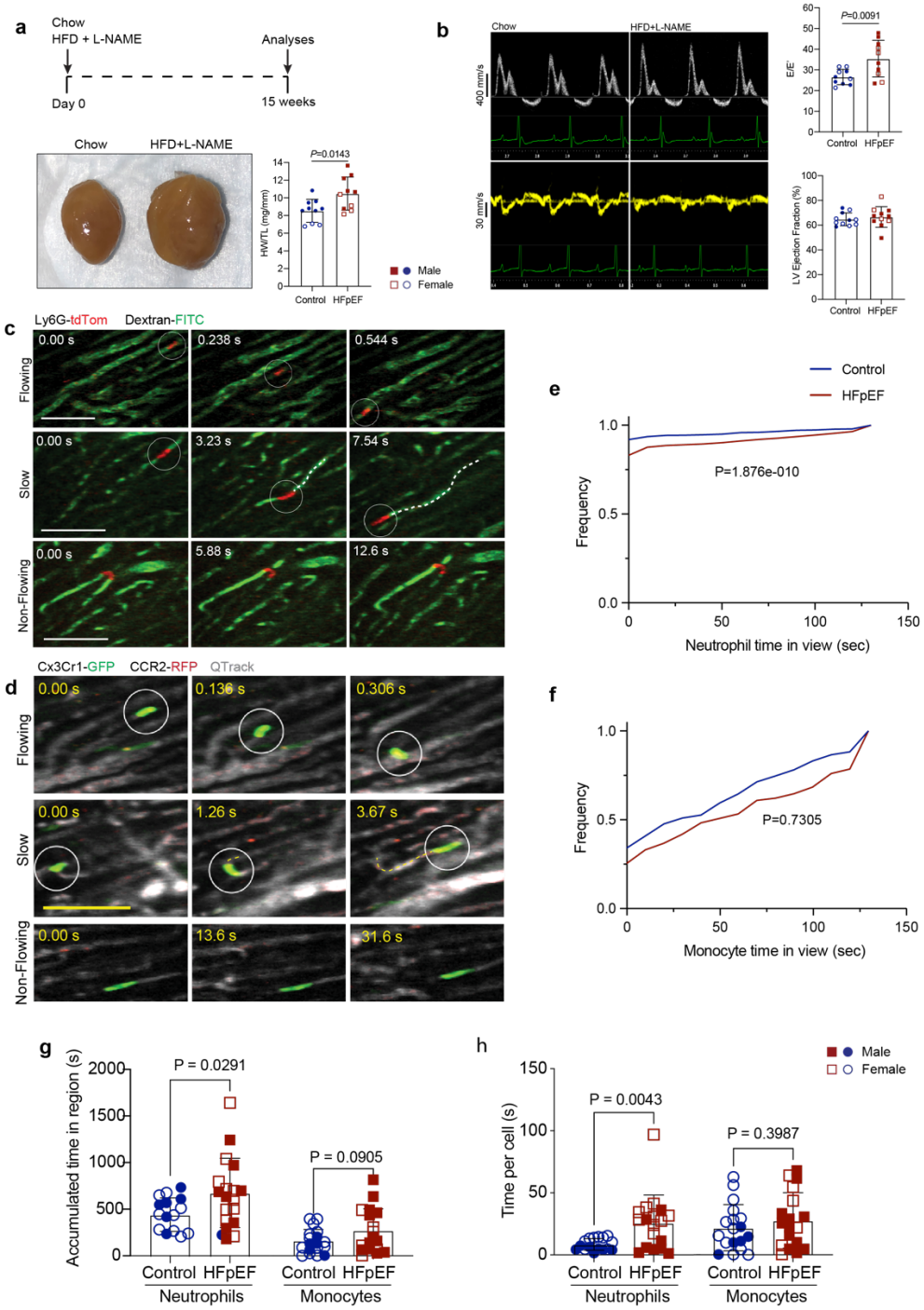

Figure 1.

Mouse models of heart failure with preserved ejection fraction (HFpEF) exhibited increased neutrophil residence in myocardial capillaries compared to control animals in C57Bl/6 mice.

(a) Schematic of HFpEF induction protocol (top). Example images (bottom left) of extracted hearts and plotted (bottom right) heart weight (HW) to tibial length (TL) ratios in control and HFpEF animals, showing cardiac hypertrophy

(b) Example echocardiography (left) and plots showing diastolic function (E/e') (top right) and left ventricular ejection fraction (bottom right) in HFpEF and control mice. Graphs include mice with labeled neutrophils or monocytes, and wild type littermates.

(c) In vivo, two-photon (2P) microscopy images of the ventricular wall in “Catchup” mice expressing tdTomato with the Ly6G promoter, a neutrophil surface marker. Intravascular FITC dextran in blood plasma (green), Ly6G+ neutrophils (red). Scale bar = 100 μm.
(d) 2P microscopy in mice expressing red fluorescent protein driven by the CCR2 promoter and green fluorescent protein with the Cx3Cr1 promoter in monocytes. Blood plasma labeled with quantum dots (Qtrack. white). Scale bar = 100 μm.
(e) Distributions of time spent in visible region of image stack by labeled neutrophils visulalized by Ly6G - tdTomato, Kolmorov-Smirnov test.
(f) Accumulated time in which a neutrophil or monocyte was visible in image stack summed over all cells in each stack visualized by Cx3Cr1-GFPm Kolmorov-Smirnov test.
(g) Average time in visible region for individual neutrophils or (h) monocytes. Control/neutrophils n = 6 mice, HFpEF/neutrophils n = 4, Control/monocytes n = 4, HFpEF/monocytes n = 6. Each dot in (e-g) represents an image stack. Indicated p-values are for Student’s t-test unless otherwise noted.

We focused on neutrophil stalls because of the larger accumulated time in capillaries compared to monocytes and clear effect of HFpEF on the distribution of visible cells. Although the average visible time duration of each individual monocyte was greater than that of an individual neutrophil, monocyte stalls occurred less frequently. The number of neutrophils visible for ≥ 100 seconds, or “stalled”, doubled in HFpEF versus control (Fig. 2a). Correspondingly, the incidence of “flowing” neutrophils with times < 5s was lower in HFpEF mice because HFpEF transit times were shifted towards slower time (Fig. 2b-c). Although there are reports of loss of capillaries in HFpEF, we found total capillary length measured in z-projections spanning 20-μm of the imaging volumes to be similar in HFpEF and control (Fig 2d-e). Total neutrophil number per time normalized by capillary lengths were also similar in HFpEF and control (Fig. 2f). The total time for which neutrophils were visible was greater in HFpEF than controls and there were fewer cells per minute, suggesting HFpEF neutrophils obstruct capillaries for longer durations than in healthy mice. On the whole, neutrophils were stalled and slowed in capillaries more in HFpEF than in control mice One interstitial neutrophil was identified during in vivo imaging out of all neutrophils counted. To further identify interstitial neutrophils, we collected tissues and used immunolabeling against tdTomatoand quantified neutrophils in ventricular tissue sections. Cryoinfarction was used as a positive control. While there was a trend towards an increase in the number of total and interstitial neutrophils HFpEF mice, this elevation is negligible compared to the number of interstitial neutrophils adjacent to an infarction[29,33-36] (Fig. 2g-i).

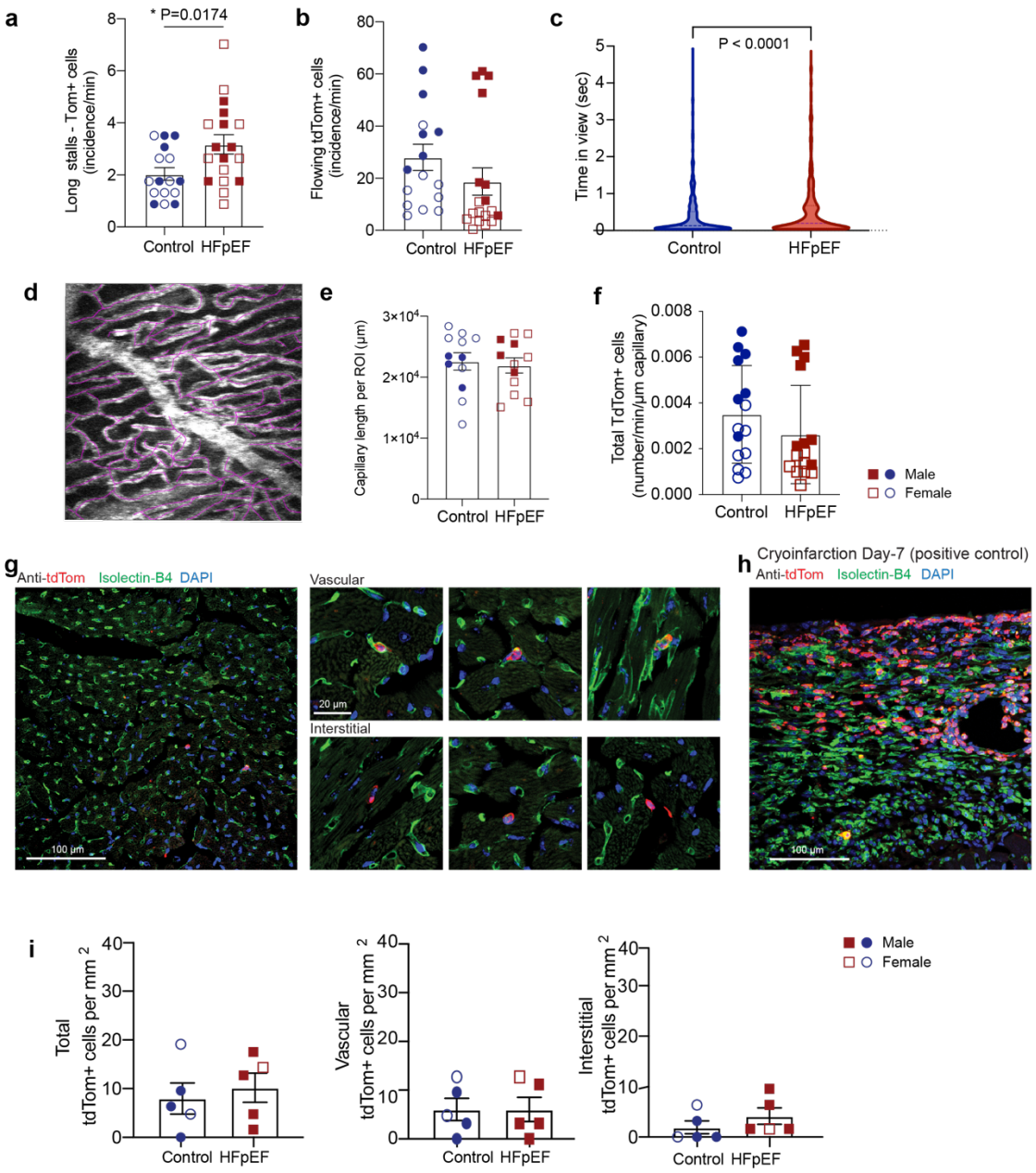

Figure 2. Characterization of neutrophils in capillaries of Catchup mice expressing tdTomato in neutrophils with HFpEF.

(a) Number of neutrophils per time visible in two-photon microscopy image stacks for 100 s or longer (categorized as long stalls) or (b) visible for <5s (categorized as flowing).

(c) Distributions of time visible of flowing neutrophils.

(d) Capillaries were traced in 20 µm projections of images from two photon image stacks to calculate (e) summed linear length of capillaries.

(f) Incidence of neutrophils observed in an image stack normalized by total capillary length.

(g) Example images of neutrophils imaged in sectioned tissue detected by an antibody against tdTomato (anti-tdTom). Vessel wall labeled with isolectin-B4 and nuclei with DAPI. Neutrophils were categorized as vascular when they were adjacent to isolectinB4 labeled vasculature and as interstitial when no contact was observed

(h) Left ventricular tissue collected 7-days after a cyroinfarct served as a positive control for histological neutrophil labeling.

(i) Quantification of all visible, vascular and interstitial neutrophils with anti-tdTom in tissue sections in control and HFpEF mice.

Hypoxia, diastolic function, and fibrosis are rescued by depleting neutrophils for 4 weeks in late stages of HFpEF. We tested the effects of long-term removal of stalls via neutrophil depletion (α-Ly6G, 2-every 3 days)[37] at late stages of the disease (last 4 weeks of the 15-week HFpEF protocol) and compared to isotype antibodies (Iso) as control with same timing and dosage (Fig. 3, control in Supplementary Fig. 4). α-Ly6G treatment did not improve hypertrophy, as assayed by heart weight/tibia length, left ventricular ejection fraction and indicators of pulmonary edema compared to control (Fig. 3c-e). However, diastolic function measured by E/e', recovered to levels near that of sham animals (Fig. 3f), while α-Ly6G treatment in control animals had no impact. Myocardial hypoxia, measured by the pimonidazole immunoassay, increased in HFpEF hearts to 150% of control (Figure 3g; Supplementary Figure 4). We found that 4-week treatment with α-Ly6G reduced hypoxia compared to control treatment and nearly attained the levels of healthy mice (Fig. 3g-h). Collagen, as assessed by Masson's Trichrome, was increased in HFpEF animals relative to control, and reduced with α-Ly6G, although not quite to the level of control (Fig. 3i-j).

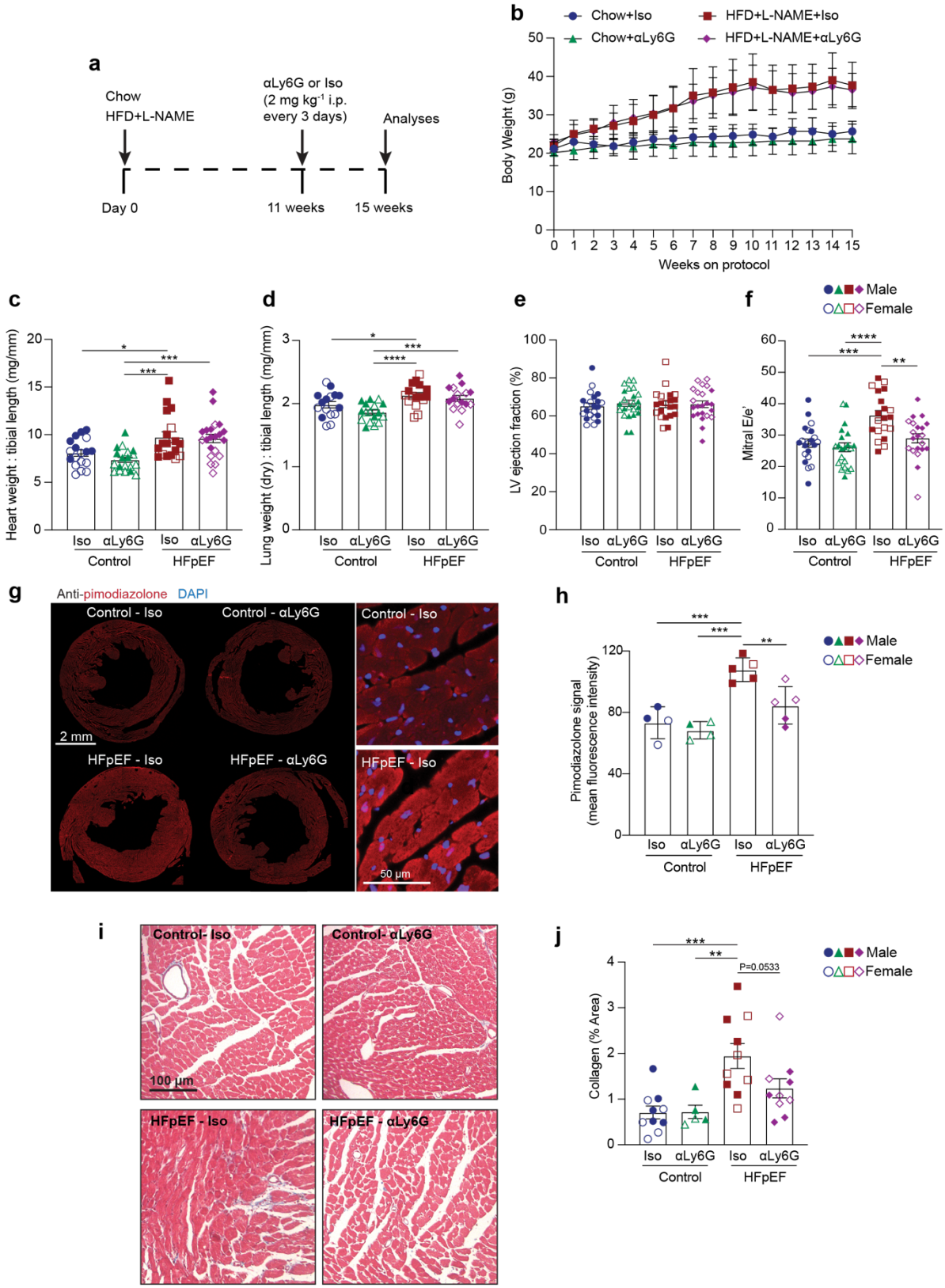
a
Chow
HFD+L-NAME
αLy6G or Iso
(2 mg kg-1 i.p.
every 3 days)
Analyses
Day 0
11 weeks
15 weeks
b
Chow+Iso
Chow+αLy6G
HFD+L-NAME+Iso
HFD+L-NAME+αLy6G
Body Weight (g)
Weeks on protocol
c
Heart weight : tibial length (mg/mm)
d
Lung weight (dry) : tibial length (mg/mm)
e
LV ejection fraction (%)
f
Mitral E/e'
Male
Female
Iso
αLy6G
Control
HFpEF
g
Anti-pimodiazolone DAPI
Control - Iso
Control - αLy6G
HFpEF - Iso
HFpEF - αLy6G
2 mm
50 µm
h
Pimodiazolone signal
(mean fluorescence intensity)
i
Control- Iso
Control- αLy6G
HFpEF - Iso
HFpEF - αLy6G
100 µm
j
Collagen (% Area)
P=0.0533

Figure 3. Extended neutrophil depletion improves diastolic function and fibrosis, but not hypertrophy.

(a) Animals received high fat diet (HFD) and L-NAME for HFpEF induction (HFpEF), while control animals received normal chow and water (healthy control) for 15 weeks. Starting at week 11, animals were injected with antibodies against Ly6G (α-Ly6G) or a nonspecific isotype control antibody (Iso) every three days until imaging and tissue collection.

(b) Animal weights starting from initiation of HFpEF or control protocols.

(c) Heart weight and (d) dry lung weight normalized to tibial length at the end of treatment period HFpEF and Chow mice treated with α-Ly6G or Iso antibodies.

(e) Echocardiography for left ventricular (LV) ejection fraction and (f) mitral E/e' at the end of treatment time for each group.

(g) Example fluorescence microscopy of sections from animals injected with a marker of hypoxia (pimonidazole) and h) quantification of labeling with antibodies against pimonidazole.

(h) Masson's Trichrome staining in tissue sections showing collagen with j) quantification of labeling at the end of the treatment period.

(Student's t-test, * $p<0.05$, ** $p<0.005$, ***$p<0.00050$

Acute neutrophil depletion in late stage HFpEF rescues hypoxia, diastolic function, and reduces stalled capillaries. We tested the effects of acute depletion for only 1-day at an advanced stage of HFpEF. Using flow cytometry, we found that αLy6G (4 mg kg^{-1}, Fig. 4a) led to a 54% reduction in systemic circulating neutrophils by 24h compared to mice administered an isotype control antibody (Figure 4b-c). We took advantage of this rapidity to isolate the effects of neutrophil depletion from possible slower changes at the end of the 15-week HFpEF induction (or control) in Catchup mice. Repeated echocardiography before and 1 day after αLy6G treatment revealed that treatment reduced E/e' in HFpEF to the same value as in control mice, while HFpEF mice receiving isotype and Chow mice receiving αLy6G did not change (Fig. 4d). Myocardial hypoxia, measured by the pimonidazole immunoassay, increased by 1.5 fold in HFpEF hearts compared to controls (Figure 4e-f). One day following αLy6G administration, pimonidazole labeling decreased in HFpEF mice compared to control treatment, approaching the levels found in mice without HFpEF induction. Intravital cardiac two-photon microscopy in Catchup mice with 15-week HFpEF induction showed that 1 day after αLy6G the rate of neutrophils appearing in image stacks was reduced to less than half the rate with the isotype antibody (Fig. 4h).

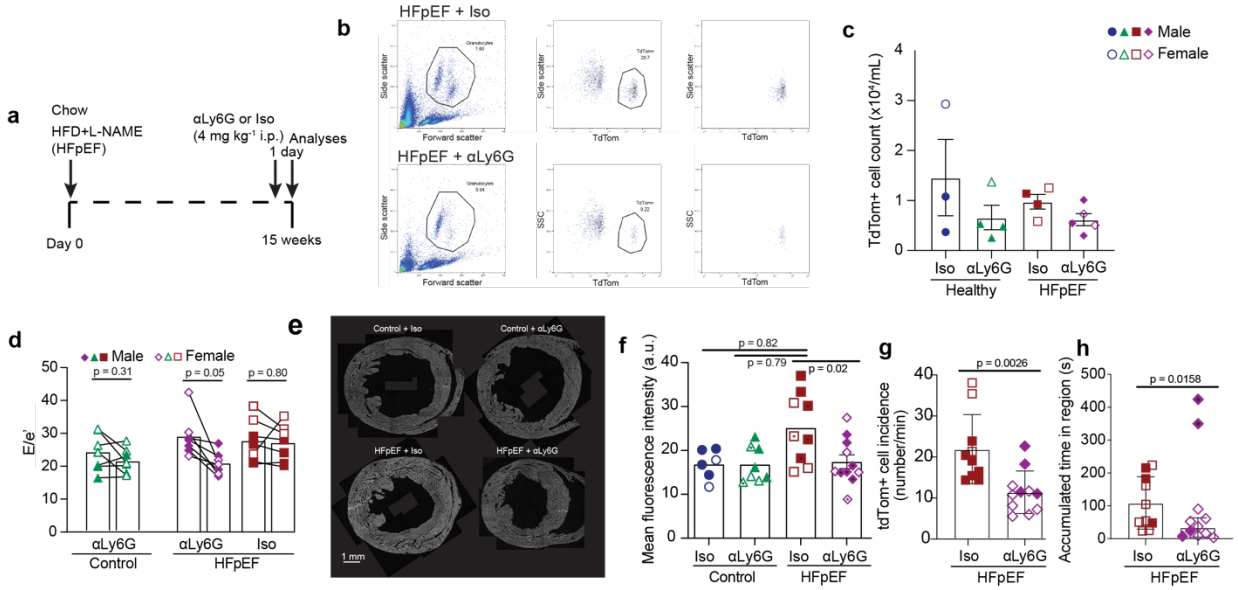

Figure 4. Acute, 1-day neutrophil depletion improves diastolic function and hypoxia and reduces neutrophil obstruction in capillaries.

(a) Animals received high fat diet and L-NAME for HFpEF induction (HFpEF), while control animals received normal chow and water for 15 weeks. One day before imaging and tissue collection animals were injected with antibodies against Ly6G (αLy6G) or an isotope, nonspecific antibody as control (Iso). (n = 3-4 per group)

(b) Flow cytometry gated on tdTomato (tdTom) was used to (c) quantify depletion of circulating neutrophils in blood from Catchup mice after 1 day of treatment with anti-Ly6G or isotype antibodies.
(d) Echocardiography performed before and 1 day after anti-Ly6G or isotype control in HFpEF and healthy mice to measure diastolic function with E/e'. Paired t-tests, healthy: n = 6, HFpEF-aly6G: n = 7, HFpEF-Iso: n = 6.
(f) Example fluorescence microscopy of sections from animals injected with a marker of hypoxia (pimonidazole) and (g) quantification of labeling with antibodies against pimonidazole.
(g) In vivo two-photon microscopy of Catchup mice was used to quantify the incidence of tdTomato-expressing (tdTom) neutrophils and (h) the sum of times a neutrophil was visible in image stacks 1 day after anti-Ly6G or isotype injection. (n = 5-6 mice). Each dot represents an image stack.

DISCUSSION

Capillary occlusions drive hypoxia in HFpEF. While many have speculated that microvascular dysfunction contributes to the heart failure, the mechanism has been elusive in part because it was difficult to visualize. Recently developed intravital two-photon microscopy enables imaging of blood flow in myocardial capillaries. In a mouse model of HFpEF, this imaging revealed that a subset of capillaries were transiently occluded primarily by arrested neutrophils that stall or slow blood flow (Fig. 1). This dynamic phenomenon was not reflected in histological counts of neutrophils in vessels and involves a tiny fraction of the number of neutrophils recruited to tissues after acute injuries such as infarctions (Fig. 2), explaining why it may not have been recognized previously. In HFpEF, the improvement of a marker of hypoxia just 24 hours after a single treatment of anti-Ly6G (Fig. 4) suggests that the presence of stalled and slowed neutrophils is detrimental.

Diastolic function is rescued independently of remodeling and hypertrophy. Diastolic function also improved with the acute, 1-day treatment to reduce neutrophil plugging of capillaries, providing benefits similar in magnitude to an extended 4-week treatment. Both long and acute treatment improved E/e' to the levels of healthy, sham-treatment mice, but the 4-week treatment also had an additional benefit of reducing fibrosis, as measured by collagen staining. Although conventional wisdom suggests that remodeling and the accumulation of fibrosis drives the inability to relax by increasing tissue stiffness, the success of the acute treatment suggests a myocardial relaxation mechanism related to blood flow improvement. One possibility that relates diastolic stiffness to hypoxia on a fast time scale is the fact that low oxygenation can impair the conversion from ADP to ATP and high ADP levels can impair crossbridge detachment, prevent acti-myosin unbinding[38]. Reminiscent of the results here, we recently discovered using similar two-photon microscopy to this work, that a tiny fraction of capillaries (1-2%) in the brains of Alzheimer's mouse models are stalled by arrested neutrophils, and this leads to a 25% decrement in brain blood flow[39]. This flow reduction was sufficient to contribute to cognitive dysfunction, demonstrated by the extremely rapid (3 hrs) onset[39] of short-term memory rescue caused by reducing the capillary stalls with α-Ly6G (same as used in this study). In both the Alzheimer's and HFpEF models, long-term treatment even at late stages resulted in sustained functional improvement [40,41]. The two parallel results suggests that the cumulative effects of distributed microscale occlusions can have large impacts on overall organ function and that at least some of effects can be rapidly reversed without restructuring of tissue. Blood flow changes from capillary dysfunction is sufficient to drive disease symptoms.

Evidence from patients and experimental work provide support for neutrophil plugging of capillaries. Patient samples show elevated expression of the adhesion markers ICAM1, VCAM1, and E-selectin[16,17,42], which could contribute to the arrest and slow flow of white blood cells in myocardial capillaries. HFpEF patient samples also show capillary rarefication[12], suggesting endothelial cell damage that could drive white cell arrest[43]. Molecular methods implicate reactive oxygen species (ROS) and downstream signaling in cardiomyocytes and fibroblasts[15,44]. ROS also affect endothelial cells and drive increased inflammation as seen through increased expression of adhesion molecules[17,42] and changes in barrier function[45]. In HFpEF patients, the neutrophil to lymphocyte ratio, a marker of inflammation, correlated with poor prognosis[46]. Myeloperoxidase (MPO) levels were increased in HFpEF patients, also suggesting an involvement of neutrophils[47]. Neutrophil depletion can have deleterious consequences after a myocardial infarction[48], suggesting that after acute injury, neutrophil "clean up" roles may be

critical[49]. However, it has also been shown that depleting neutrophils in the pressure overload model of HFrEF can prevent heart failure[20]. The link between neutrophils and fibrosis is supported by additional work in mice. Zhang, et al. found similarly improved E/e' and fibrosis without rescue of myocardial size in a different model of HFpEF after SGLT2 inhibition with dapagliflozin[50]. They implicated neutrophils in this study, by interfering with neutrophil extracellular traps (NETs), inhibition of high mobility group protein B1 (HMGB1), and by directly degrading NETs with deoxyribonuclease 1 and finding the same changes.

Future work. Follow up studies exploring the idea that perfusion deficits caused by capillary stalls can drive key symptoms are needed to address some of the limitations in this study. While α-Ly6G is useful as experimental tool, because it is not a human protein, further exploration for better translational targets is critical. While there is some concern that depletion by this antibody was not a complete elimination of all types of neutrophils[51], our results in both the heart and the Alzheimer's disease brain[39-41] show substantial improvements in multiple physiological parameters suggesting that this manipulation is sufficient to motivate further work on better strategies. A similar phenomenon of stalled and slowed capillaries in an alternative model of heart failure ApoE$^{-/-}$ with high fat diet, suggests that this phenomenon is not an artifact of the HFpEF model (Supplementary Figs. 2-3). We did not find notable sex dependence in the incidence of neutrophil stalls or recovery with depletion, but this study was not powered to resolve sex differences. Further study, especially using menopause models for females, will be critical in assessing the translational importance of these results.

CONCLUSION

This work points to a novel mechanism implicating capillaries that drives the symptoms of diastolic dysfunction in HFpEF. Elimination of neutrophils that obstructed capillaries decreased hypoxia, prevented fibrosis, and decreased ventricular stiffness to improve diastolic function. Because neutrophil adherence to endothelium is the first step in inflammation, such capillary stalling with little neutrophil tissue extravasation is likely in many diseases, especially those involving chronic inflammation. While this suggests new targets for future drugs, it also is possible that many drugs either directly or indirectly improve capillary stalling so that the therapeutic effect is largely pleiotropic.

METHODS

See separate online methods

REFERENCES

1 Borlaug, B. A. The pathophysiology of heart failure with preserved ejection fraction. *Nat Rev Cardiol* **11**, 507-515, doi:10.1038/nrcardio.2014.83 (2014).

2 Massie, B. M. *et al.* Irbesartan in patients with heart failure and preserved ejection fraction. *N Engl J Med* **359**, 2456-2467, doi:10.1056/NEJMoa0805450 (2008).

3 Yusuf, S. *et al.* Effects of candesartan in patients with chronic heart failure and preserved left-ventricular ejection fraction: the CHARM-Preserved Trial. *Lancet* **362**, 777-781, doi:10.1016/S0140-6736(03)14285-7 (2003).

4 Anker, S. D. *et al.* Empagliflozin in Heart Failure with a Preserved Ejection Fraction. *The New England journal of medicine* **385**, 1451-1461, doi:10.1056/NEJMoa2107038 (2021).

5 Kato, S. *et al.* Impairment of Coronary Flow Reserve Evaluated by Phase Contrast Cine-Magnetic Resonance Imaging in Patients With Heart Failure With Preserved Ejection Fraction. *J Am Heart Assoc* **5**, doi:10.1161/JAHA.115.002649 (2016).

6 Srivaratharajah, K. *et al.* Reduced Myocardial Flow in Heart Failure Patients With Preserved Ejection Fraction. *Circ Heart Fail* **9**, doi:10.1161/CIRCHEARTFAILURE.115.002562 (2016).

7 Shah, S. J. *et al.* Prevalence and correlates of coronary microvascular dysfunction in heart failure with preserved ejection fraction: PROMIS-HFpEF. *European heart journal* **39**, 3439-3450, doi:10.1093/eurheartj/ehy531 (2018).
8 Dryer, K. *et al.* Coronary microvascular dysfunction in patients with heart failure with preserved ejection fraction. *American journal of physiology. Heart and circulatory physiology* **314**, H1033-H1042, doi:10.1152/ajpheart.00680.2017 (2018).
9 Obokata, M. *et al.* Myocardial Injury and Cardiac Reserve in Patients With Heart Failure and Preserved Ejection Fraction. *J Am Coll Cardiol* **72**, 29-40, doi:10.1016/j.jacc.2018.04.039 (2018).
10 Mohammed, S. F. *et al.* Coronary microvascular rarefaction and myocardial fibrosis in heart failure with preserved ejection fraction. *Circulation* **131**, 550-559, doi:10.1161/CIRCULATIONAHA.114.009625 (2015).
11 Schiattarella, G. G. *et al.* Nitrosative stress drives heart failure with preserved ejection fraction. *Nature* **568**, 351-356, doi:10.1038/s41586-019-1100-z (2019).
12 Zeng, H. & Chen, J. X. Microvascular Rarefaction and Heart Failure With Preserved Ejection Fraction. *Front Cardiovasc Med* **6**, 15, doi:10.3389/fcvm.2019.00015 (2019).
13 AbouEzzeddine, O. F. *et al.* Myocardial Energetics in Heart Failure With Preserved Ejection Fraction. *Circ Heart Fail* **12**, e006240, doi:10.1161/CIRCHEARTFAILURE.119.006240 (2019).
14 Lyle, M. A., Alabdaljabar, M. S., Han, Y. S. & Brozovich, F. V. The vasculature in HFpEF vs HFrEF: differences in contractile protein expression produce distinct phenotypes. *Heliyon* **6**, e03129, doi:10.1016/j.heliyon.2019.e03129 (2020).
15 D'Amario, D. *et al.* Microvascular Dysfunction in Heart Failure With Preserved Ejection Fraction. *Front Physiol* **10**, 1347, doi:10.3389/fphys.2019.01347 (2019).
16 Franssen, C. *et al.* Myocardial Microvascular Inflammatory Endothelial Activation in Heart Failure With Preserved Ejection Fraction. *JACC Heart Fail* **4**, 312-324, doi:10.1016/j.jchf.2015.10.007 (2016).
17 Westermann, D. *et al.* Cardiac inflammation contributes to changes in the extracellular matrix in patients with heart failure and normal ejection fraction. *Circ Heart Fail* **4**, 44-52, doi:10.1161/CIRCHEARTFAILURE.109.931451 (2011).
18 Paulus, W. J. & Tschope, C. A novel paradigm for heart failure with preserved ejection fraction: comorbidities drive myocardial dysfunction and remodeling through coronary microvascular endothelial inflammation. *J Am Coll Cardiol* **62**, 263-271, doi:10.1016/j.jacc.2013.02.092 (2013).
19 Hulsmans, M. *et al.* Cardiac macrophages promote diastolic dysfunction. *J Exp Med* **215**, 423-440, doi:10.1084/jem.20171274 (2018).
20 Wang, Y. *et al.* Wnt5a-Mediated Neutrophil Recruitment Has an Obligatory Role in Pressure Overload-Induced Cardiac Dysfunction. *Circulation* **140**, 487-499, doi:10.1161/CIRCULATIONAHA.118.038820 (2019).
21 Devi, S. *et al.* Multiphoton imaging reveals a new leukocyte recruitment paradigm in the glomerulus. *Nat Med* **19**, 107-112, doi:10.1038/nm.3024 (2013).
22 Ahn, S. J., Anrather, J., Nishimura, N. & Schaffer, C. B. Diverse Inflammatory Response After Cerebral Microbleeds Includes Coordinated Microglial Migration and Proliferation. *Stroke; a journal of cerebral circulation* **49**, 1719-1726, doi:10.1161/STROKEAHA.117.020461 (2018).
23 McDonald, B. *et al.* Intravascular danger signals guide neutrophils to sites of sterile inflammation. *Science* **330**, 362-366, doi:10.1126/science.1195491 (2010).
24 Cruz Hernandez, J. C. *et al.* Neutrophil adhesion in brain capillaries reduces cortical blood flow and impairs memory function in Alzheimer's disease mouse models. *Nat Neurosci* **22**, 413-420, doi:10.1038/s41593-018-0329-4 (2019).
25 Neupane, A. S. & Kubes, P. Imaging reveals novel innate immune responses in lung, liver, and beyond. *Immunol Rev* **306**, 244-257, doi:10.1111/imr.13040 (2022).
26 Allan-Rahill, N. H., Lamont, M. R. E., Chilian, W. M., Nishimura, N. & Small, D. M. Intravital Microscopy of the Beating Murine Heart to Understand Cardiac Leukocyte Dynamics. *Front Immunol* **11**, 92, doi:10.3389/fimmu.2020.00092 (2020).
27 Jones, J. S., Small, D. M. & Nishimura, N. In Vivo Calcium Imaging of Cardiomyocytes in the Beating Mouse Heart With Multiphoton Microscopy. *Front Physiol* **9**, 969, doi:10.3389/fphys.2018.00969 (2018).
28 Lee, S. *et al.* Real-time in vivo imaging of the beating mouse heart at microscopic resolution. *Nature communications* **3**, 1054, doi:10.1038/ncomms2060 (2012).

29 Kavanagh, D. P. J., Lokman, A. B., Neag, G., Colley, A. & Kalia, N. Imaging the injured beating heart intravitally and the vasculoprotection afforded by haematopoietic stem cells. *Cardiovascular research* **115**, 1918-1932, doi:10.1093/cvr/cvz118 (2019).
30 Jung, S. *et al.* Analysis of fractalkine receptor CX(3)CR1 function by targeted deletion and green fluorescent protein reporter gene insertion. *Molecular and cellular biology* **20**, 4106-4114 (2000).
31 Saederup, N. *et al.* Selective chemokine receptor usage by central nervous system myeloid cells in CCR2-red fluorescent protein knock-in mice. *PloS one* **5**, e13693, doi:10.1371/journal.pone.0013693 (2010).
32 Auffray, C. *et al.* Monitoring of blood vessels and tissues by a population of monocytes with patrolling behavior. *Science* **317**, 666-670, doi:10.1126/science.1142883 (2007).
33 Bajpai, G. *et al.* Tissue Resident CCR2- and CCR2+ Cardiac Macrophages Differentially Orchestrate Monocyte Recruitment and Fate Specification Following Myocardial Injury. *Circulation research* **124**, 263-278, doi:10.1161/CIRCRESAHA.118.314028 (2019).
34 Jung, K. *et al.* Endoscopic time-lapse imaging of immune cells in infarcted mouse hearts. *Circulation research* **112**, 891-899, doi:10.1161/CIRCRESAHA.111.300484 (2013).
35 Li, W. *et al.* Intravital 2-photon imaging of leukocyte trafficking in beating heart. *The Journal of clinical investigation* **122**, 2499-2508, doi:10.1172/JCI62970 (2012).
36 Matsuura, R. *et al.* Intravital imaging with two-photon microscopy reveals cellular dynamics in the ischeamia-reperfused rat heart. *Scientific reports* **8**, doi:ARTN 15991 10.1038/s41598-018-34295-w (2018).
37 Erdener, S. E. *et al.* Dynamic capillary stalls in reperfused ischemic penumbra contribute to injury: A hyperacute role for neutrophils in persistent traffic jams. *Journal of cerebral blood flow and metabolism : official journal of the International Society of Cerebral Blood Flow and Metabolism* **41**, 236-252, doi:10.1177/0271678X20914179 (2021).
38 Sequeira, V. *et al.* Synergistic role of ADP and Ca(2+) in diastolic myocardial stiffness. *J Physiol* **593**, 3899-3916, doi:10.1113/JP270354 (2015).
39 Cruz Hernandez, J. C. *et al.* Neutrophil adhesion in brain capillaries reduces cortical blood flow and impairs memory function in Alzheimer's disease mouse models. *Nature neuroscience*, doi:10.1038/s41593-018-0329-4 (2019).
40 Ali, M. *et al.* Inhibition of peripheral VEGF signaling rapidly reduces leucocyte obstructions in brain capillaries and increases cortical blood flow in an Alzheimer's disease mouse model. *bioRxiv*, 2021.2003.2005.433976, doi:10.1101/2021.03.05.433976 (2021).
41 Bracko, O. *et al.* Increasing cerebral blood flow improves cognition into late stages in Alzheimer's disease mice. *Journal of cerebral blood flow and metabolism : official journal of the International Society of Cerebral Blood Flow and Metabolism* **40**, 1441-1452, doi:10.1177/0271678X19873658 (2020).
42 van Heerebeek, L. *et al.* Diastolic stiffness of the failing diabetic heart: importance of fibrosis, advanced glycation end products, and myocyte resting tension. *Circulation* **117**, 43-51, doi:10.1161/CIRCULATIONAHA.107.728550 (2008).
43 Reeson, P., Choi, K. & Brown, C. E. VEGF signaling regulates the fate of obstructed capillaries in mouse cortex. *Elife* **7**, doi:10.7554/eLife.33670 (2018).
44 Camici, P. G., Tschope, C., Di Carli, M. F., Rimoldi, O. & Van Linthout, S. Coronary microvascular dysfunction in hypertrophy and heart failure. *Cardiovascular research* **116**, 806-816, doi:10.1093/cvr/cvaa023 (2020).
45 Zhu, L. & He, P. fMLP-stimulated release of reactive oxygen species from adherent leukocytes increases microvessel permeability. *American journal of physiology. Heart and circulatory physiology* **290**, H365-372, doi:10.1152/ajpheart.00812.2005 (2006).
46 Boralkar, K. A. *et al.* Value of Neutrophil to Lymphocyte Ratio and Its Trajectory in Patients Hospitalized With Acute Heart Failure and Preserved Ejection Fraction. *The American journal of cardiology* **125**, 229-235, doi:10.1016/j.amjcard.2019.10.020 (2020).
47 Hage, C. *et al.* Myeloperoxidase and related biomarkers are suggestive footprints of endothelial microvascular inflammation in HFpEF patients. *ESC Heart Fail* **7**, 1534-1546, doi:10.1002/ehf2.12700 (2020).
48 Kain, V. & Halade, G. V. Role of neutrophils in ischemic heart failure. *Pharmacol Ther* **205**, 107424, doi:10.1016/j.pharmthera.2019.107424 (2020).

49 Kolaczkowska, E. & Kubes, P. Neutrophil recruitment and function in health and inflammation. *Nat Rev Immunol* **13**, 159-175, doi:10.1038/nri3399 (2013).
50 Zhang, X. L. *et al.* HMGB1-Promoted Neutrophil Extracellular Traps Contribute to Cardiac Diastolic Dysfunction in Mice. *J Am Heart Assoc* **11**, e023800, doi:10.1161/JAHA.121.023800 (2022).
51 Iliakis, C. S. & Wack, A. Never trust a single myeloid marker: Ly6G on repair-promoting lung macrophages. *Sci Immunol* **9**, eadq7306, doi:10.1126/sciimmunol.adq7306 (2024).